

UC San Diego

UC San Diego Electronic Theses and Dissertations

Title

Immunologic evolution in nonmelanoma skin cancer development

Permalink

<https://escholarship.org/uc/item/5r94h5d8>

Author

Jaljuli, Malak

Publication Date

2021

Peer reviewed|Thesis/dissertation

UNIVERSITY OF CALIFORNIA SAN DIEGO

Immunologic evolution in nonmelanoma skin cancer development

A Thesis submitted in partial satisfaction of the requirements for the degree Master of Science

in

Biology

by

Malak Jaljuli

Committee in charge:

Professor Gregory A Daniels, Chair
Professor Ananda Goldrath, Co-Chair
Professor Steve Briggs
Professor Ella Tour

The Thesis of Malak Jaljuli is approved, and it is acceptable quality and form for publication of microfilm and electronically.

University of California San Diego

2021

TABLE OF CONTENTS

Thesis Approval Page	iii
Table of Contents.....	iv
List of Tables.....	v
List of Figures.....	vi
List of Supplemental Tables.....	vii
List of Supplemental Figures	viii
Acknowledgements.....	ix
Abstract of the Thesis.....	x
Introduction.....	1
Review.....	3
Preliminary Work.....	9
Materials and Methods.....	14
Results.....	18
Discussion.....	27
Tables	37
Supplemental Tables.....	45
Supplemental Figures	46
Bibliography.....	48

LIST OF TABLES

Table 1: Table of significantly differentially expressed genes and the pathways in which they are involved when comparing actinic keratosis to squamous cell in situ in non-transplant patients.	37
Table 2: Table of significantly differentially expressed genes and the pathways in which they are involved when comparing normal skin to squamous cell in situ in non-transplant patients.	38
Table 3: Table of significantly differentially expressed genes and the pathways in which they are involved when comparing normal skin to invasive squamous cell carcinoma in non-transplant patients.	39
Table 4: Table of significantly differentially expressed genes and the pathways in which they are involved when comparing normal skin to moderately differentiated and high risk squamous cell carcinoma in non-transplant patients.	40
Table 5: Table of significantly differentially expressed genes and the pathways in which they are involved when comparing normal skin to actinic keratosis in organ transplant patients.	41
Table 6: Table of significantly differentially expressed genes and the pathways in which they are involved when comparing actinic keratosis to squamous cell in situ in organ transplant patients.	42
Table 7: Table of significantly differentially expressed genes and the pathways in which they are involved when comparing squamous cell in situ to invasive squamous cell carcinoma in organ transplant patients.	43
Table 8: Table of significantly differentially expressed genes and the pathways in which they are involved when comparing normal skin to squamous cell in situ in organ transplant patients.	44

LIST OF FIGURES

Figure 1: Heat map showing an upregulation of 19 hedgehog signaling pathway genes in basal cell carcinoma (BCC) samples that is not matched in the squamous cell carcinoma (SCC) samples.	13
--	----

LIST OF SUPPLEMENTAL TABLES

Supplemental Table 1: Undirected global significance scores in SCC vs. BCC show that hedgehog signaling is the most differentially expressed gene set, whereas directed global significance scores show the most upregulated gene sets in SCC when compared to BCC are the myeloid compartment, interferon signaling, cytotoxicity, and antigen presentation. 45

LIST OF SUPPLEMENTAL FIGURES

Supplemental Figure 1: Plot of pathway score variation from non-transplant actinic keratosis to non-transplant squamous cell in situ shows increased expression in the majority of the genes that make up the cell proliferation pathway in squamous cell in situ compared to actinic keratosis. 46

Supplemental Figure 2: Plot of pathway score variation from non-transplant normal skin to non-transplant invasive squamous cell carcinoma shows increased expression in the majority of the genes that make up the matrix remodeling and metastasis, the metabolic stress, the cell proliferation, and the cytotoxicity pathways in invasive squamous cell carcinoma compared to normal skin. 47

ACKNOWLEDGMENTS

I would like to acknowledge Professor Gregory Daniels for his guidance as the chair of my committee. I would also like to thank Dr. Stephen Schoenberger and the members of the Schoenberger lab for giving me a space to conduct my experiments as well as advice throughout my research. I would like to thank Dr. Brian Hinds for his contribution in both the pilot study, as well as my masters thesis, and providing the samples needed for this research. I would also like to thank Dr. Elsa Molina for her collaboration in both the pilot study, as well as my masters thesis, in helping me with both the experimental protocol as well as the data analysis. I would like to thank Professor Ella Tour for her support and motivation throughout the entire process of writing my thesis. I want to thank my committee members, Professor Ananda Goldrath and Professor Steve Briggs, for their direction as well. Finally, I want to thank The Program in Immunology for awarding us the Collaborative Pilot Grant to conduct this study.

ABSTRACT OF THE THESIS

Immunologic evolution in nonmelanoma skin cancer development

by

Malak Jaljuli

Master of Science in Biology

University of California San Diego, 2021

Professor Gregory Daniels, Chair
Professor Ananda Goldrath, Co-Chair

Patients with metastatic and locally advanced cutaneous squamous cell carcinoma (CuSCC) undergoing anti-programmed death-1 (PD-1) immune checkpoint blockade therapy have shown durable anti-tumor activity. Response to anti-PD-1 checkpoint blockade therapy partially depends on an existing anti-tumor T cell population within the tumor microenvironment (TME) directed against neoantigens specific for the tumor. The development and ultimately escape from this immune response is not well understood in cutaneous squamous cell cancer development. Using gene expression profiles including those that predict response to anti-PD-1 therapy, I will investigate normal skin to precancerous skin to invasive CuSCC from both immunocompetent and immunocompromised patients with quantitative molecular profiling of metabolic pathway and immune related gene expression. We expect to show differential expression of genes involved in shaping the TME and immune cell infiltration from normal skin to invasive cancer. Therefore, these findings can help identify steps in cancer development and

perhaps insight into prevention strategies. In addition, we will compare the development of tumors in the context of a normal immune system and an impaired immune response (ie organ transplant patients). We hope these profiles may help identify additional therapeutic strategies for treating both immune competent and immune suppressed patients.

Introduction

Cancer progression is not only reliant on the malignant cells themselves, but highly impacted by the other cells that are recruited to the tumor site, and their interactions with the cancer (Balkwill et al., 2012). These interactions contribute to the tumor microenvironment (TME), which not only includes the physical space surrounding the tumor bound by the scaffold of the extracellular matrix, but also all surrounding blood vessels, immune cells and signaling molecules (Balkwill et al., 2012). Therefore, the TME is considered a dynamic component of solid tumors, due to the pressures either the cancerous cells or the surrounding cells place on each other. For example, the extracellular matrix itself contains growth factors that help the cancer bring in more blood vessels to feed the tumor site, and plays a role in a cancer's metastasis (LeBleu, 2015).

Immune cells, both innate and adaptive, drive this dynamic interaction between cancer cells and the TME (Balkwill et al., 2012). Depending on the type of infiltrating cells, the result can either be immunostimulating (anti-tumor) or immunosuppressive (pro-tumor). For example, many different types of T cells can be part of the TME. Infiltrated memory or cytotoxic CD8⁺ T cells are usually associated with good prognosis since these cells are able to recognize antigens presented by dendritic cells that signal the CD8⁺ T cell to kill the tumor (Balkwill et al., 2012). Along with the CD8⁺ T cells, CD4⁺ T helper cells also contribute to tumor eradication by producing the inflammatory cytokines IL-2 and IFN- γ . Therefore, these cytokines are also correlative with a good prognosis if located inside the TME (Balkwill et al., 2012). However some CD4⁺ T cells, such as regulatory T cells, are immunosuppressive, and therefore tumor promoting (Togashi et al., 2019). Unlike CD4⁺ T helper cells, regulatory T cells normally maintain immune homeostasis by acting as a suppressive counterbalance to the immune system's

response to foreign cells. Therefore cancerous cells manipulate their function by presenting self antigens that are preferentially recognized by regulatory T cells that migrate and expand in the TME (Togashi et al., 2019). Ultimately, both the healthy body and the malignant cells act on each other to shape the cancer's progression and response to therapy.

In addition to the interactions occurring within the TME, cancer progression and response to therapy is also determined by how easy it is for immune cells to infiltrate the tumor, namely inflamed vs. non-inflamed tumors (Bonaventura et al, 2019). Patients with inflamed tumors are expected to have a better prognosis due to the interactions between the tumor and infiltrated T cells described above. The reason these tumors are infiltrated by T cells is due to the increase in their mutations that can be recognized as foreign to the immune system (Bonaventura et al, 2019). Whereas in non-inflamed tumors, immune T cells are unable to penetrate the tumor due to its unique TME, especially the increased surrounding regulatory T cells, and therefore the immune system hasn't yet recognized these tumors. One example of an inflamed tumor served by its immune cell infiltrated TME for treatment is cutaneous squamous cell carcinoma (CuSCC).

My thesis will consist of two parts, the first half will be a literature review on the tumor microenvironment in CuSCC, and its current treatments. The second half will include my masters research in the immunologic characterization of precancerous skin malignancies leading up to CuSCC and their respective microenvironment changes as determinants for cancer development and therapy response, as well as an analysis of preliminary data comparing basal cell carcinoma (BCC) to CuSCC using the same NanoString assay that is used for my masters project.

1. A Review

1.1 Cutaneous Squamous Cell Carcinoma

Cutaneous squamous cell carcinoma (CuSCC) is the second most common type of skin cancer in the U.S., and is usually treated by a simple excision of the tumor (Karia et al., 2013). However, CuSCC patients also have a risk of metastasis, therefore making it a highly aggressive and life threatening disease (Karia et al., 2013). The most common patient group is elderly patients with years of cumulative carcinogenic UV exposure (Ng et al., 2011). However, other patient groups are genetically or immunologically predisposed to develop CuSCC at a younger age with even higher rates of morbidity. These high risk groups include patients with precancerous growths such as actinic keratosis, or patients who are immunosuppressed such as organ transplant recipients (OTR). Many patients in these high risk groups die from the metastatic disease despite the surgical removal of the cancerous cells, with a 56% mortality within 3 years in OTR patients (Ng et al., 2011). However, recent studies on new therapy approaches for the treatment of metastatic and locally advanced CuSCC have only been performed on immunocompetent patients (Migden et al., 2018). Therefore, for individuals who are genetically or immunologically predisposed to develop CuSCC, there is still a lapse in establishing profiles for disease prognosis or prediction of response to the currently available therapies (Jennings et al., 2010).

1.2 Programed Cell Death and Immunotherapy

One therapy that has demonstrated a demand for establishing prognostic genetic profiles is immune checkpoint blockade therapy (Jamieson & Maker, 2017). It has been effective in

treating a subset of patients with many different types of cancer since it works by blocking major immunosuppressive pathways, such as the programmed death-1/ligand-1 (PD-1/PD-L1) pathway, that allow the cancer to hide from an immune response (Spranger & Gajewski, 2018). Under normal conditions, activated T cells express PD-1, which binds to its ligand PD-L1 expressed on many other inflammatory immune cells to promote apoptosis or anergy of cytotoxic T cells while also suppressing apoptosis of regulatory T cells (Jiang et al., 2019). Therefore, malignant cells manipulate this to over-express PD-L1 on their surface or other cells in the TME, which in turn inhibits those same cytotoxic T cells that are trying to fight the tumor, and the remaining cytotoxic T cells are inhibited in the TME. Tumor cells also have a built in positive feedback loop in which T cell exhaustion further allows the tumor to secrete pro-inflammatory cytokines that further upregulate PD-L1 on the surface of those tumor cells and so on. (Jiang et al., 2019)

Cemiplimab, an anti-PD-1 immune checkpoint blockade, was recently approved for the treatment of metastatic and locally advanced CuSCC, inducing a response in approximately 50% of patients (Migden et al., 2018). The observed durable response to this treatment has been credited to the tumors' high mutational burden caused by DNA damage from cumulative UV light exposure. This high tumor mutation burden, along with certain genetic biomarkers that the tumor expresses such as PD-L1, all factor into the tumor's tumorigenicity. However, genetic biomarkers corresponding to the tumorigenicity of the tumor do not alone provide an accurate prediction of response to therapy (Rizvi et al., 2015). According to previous studies reviewed by Rizvi and colleagues (2015), tumors that are positive for PD-L1 expression do not necessarily respond to anti-PD-1 blockade therapy, and not expressing PD-L1 in the tumor does not ultimately imply of a lack of response in CuSCC patients. Therefore, there must be another

process working in parallel to tumorigenicity; immunogenicity describes the amount of lymphocytic infiltrates into the tumor microenvironment, and consequently, the extent of anti-tumor IFN- γ cytokine signaling (Migden et al., 2018, Lee et al., 2018).

1.3 Neoantigens and their Interaction with Immunotherapy

The many different tumorigenic and immunogenic processes in the tumor all play a role in the cancer's formation of neoantigens, which are potentially tumor specific immune targets. For example, a higher tumor mutational burden likely reflects a larger number of neoantigens and a broader recognition of the tumor. (Lee et al., 2018). T cells reactive to antigens not subject to central tolerance can be found directly in the patient's blood. We infer that by being found in the patient's blood, those neoantigens have already induced a response and are targeted by the immune system as a "foreign object" (Schoenberger, 2017). One approach to target personalized neoantigens is combining different major neoantigens—preferably created by driver mutations to generate a greater response—into a vaccine, which would prime the body to specifically attack the malignant cells (Schumacher & Schreiber, 2015). However, finding those driver mutations that give rise to effective neoantigen targets can be challenging given HLA restrictions and has had limited success (Lee et al., 2018).

Many obstacles hinder developing effective personalized neoantigen vaccines. One widely studied is the ability of tumor neoantigens expression to change due to immunoediting (Efremova et al., 2017). A common model of immunoediting drives clonal evolution through three phases: the immune system's elimination of the tumor, equilibrium between the tumor and immune system where the tumor is controlled by not removed, and the tumor's escape from the immune system's radar as it acquires resistance, allowing for tumor expansion (Efremova et al.,

2017). Immunoediting occurs in the equilibrium phase where the cells that are able to resist elimination and enter equilibrium are a genetic variant of the original tumor cells (Dunn et al., 2004). The immune system's selective pressure on tumor cells is also observed during acquired resistance to checkpoint blockade therapies, with changes in the presentation of antigens or the tumor microenvironment (Efremova et al., 2017). For example, immunoediting could make the tumor more homogenous by eliminating some neoantigen mutations to allow immune escape during checkpoint blockade therapy. Therefore, while a high tumor mutational burden is being studied as a biomarker of response to immune checkpoint blockade therapy, a decrease in the tumor heterogeneity would also decrease a tumor's immunogenicity. To overcome this selective pressure, Efremova and colleagues (2017) report that neoantigen vaccines can create an immune response against new neoantigens that weren't found before the vaccination by broadening the diversity of the T cell response. Neoantigen vaccines however can also create a negative feedback loop suppressing tumor immunity by increasing T cell infiltration and IFN- γ secretion, and upregulate the PD-1/PD-L1 pathway and other immunosuppressive pathways (Efremova et al., 2017). The link between tumor mutational burden and response to immune checkpoint inhibition is complex, with studies in melanoma and non-small cell lung cancer supporting the relationship between higher tumor mutational burden and progression free survival, but studies in multiple myeloma patients showing the opposite (Borden et al., 2019) Therefore, only an increase in tumor mutational burden, and consequently the number of neoantigens, is not enough to predict response to therapy. Borden and colleagues (2019) found that homogeneity of tumor neoantigens, as well as T cell receptor recognition potential, could provide a more accurate prediction of response to immune checkpoint blockade therapies. Ultimately, monitoring the dynamic changes of tumors undergoing therapy and the development of tumors from normal

tissue may provide insights into predictive markers of response as well as determinants of tumorigenesis.

1.4 Evolution of normal skin to CuSCC

Our research hypothesizes that as tumors develop from normal skin to malignant lesions, we may observe dynamic changes from immunoediting along the continuum of pathologic changes. The selective pressure of immunoediting seen in response and in some patients resistance to therapy when tumors escape from immune checkpoint blockades, may also be observed as actinic keratoses evolve into invasive CuSCC. The link seen between actinic keratosis and CuSCC, such as 20-27% of CuSCC appear either from an actinic keratosis or close around it (Padilla et al., 2010) and around 65% of CuSCC appear from other premalignant lesions (Li et al., 2015), leads us to believe that a switch in the way the immune system views the lesion can decide whether the lesion is eliminated or in equilibrium with the immune response, or whether it can evade the immune system and evolve into a cancer. Differentially expressed genes found by Padilla and colleagues confirmed that some actinic keratosis are a precursor to CuSCC (2010). When analyzing samples from normal non-sun exposed skin, normal sun exposed skin, actinic keratosis, and CuSCC, they found the samples clustered into 2 distinct gene families, one consisting of the actinic keratosis and CuSCC samples, and the other consisting of all the normal skin samples, both non-sun exposed and sun exposed. The genes were further divided into 2 distinct gene groups, genes that were upregulated and genes that were downregulated in actinic keratosis and CuSCC compared to normal skin samples (Padilla et al., 2010). Therefore, their research supported their hypothesis that the evolution from normal to actinic keratosis to CuSCC was on a continuum of similar genetic alterations, but didn't find genes that were statistically significantly different between the steps of cancer development (Padilla et al., 2010).

Previous studies have determined risk factors that improved previous staging's ability to predict metastasis into aggressive CuSCCs; either tumor thickness, or a combination of risk factors including tumor diameter, differentiation histology, perineural invasion, and tumor invasion (Brantsch et al., 2008) (Karia et al., 2014). However, the genetic and immunologic relationship with risk factors involving the evolution of actinic keratosis into CuSCC has not yet been clearly characterized.

2. Preliminary Work

Given the challenges in obtaining fresh clinical specimens, we chose to focus on available tissue from clinical cases. Utilizing archived tissues however is limited by what is available in the archives and what techniques may be utilized. NanoString is a panel of molecular bar codes that can be utilized to quantitate 100s of molecules in a single run (nCounter PanCancer, 2021). The targets can be RNA, DNA or protein. As a preliminary study to first determine the accuracy and feasibility of applying NanoStrings to determine gene expression on archival human tumor tissue, we examined established intrinsic (hedgehog pathway) and extrinsic (interferon signaling) pathways important for tumor development and response to therapy. CuSCC and basal cell carcinomas were chosen as ideal tumors to validate my methods. Both keratinocyte derived tumors are common, both occur due to UV damage and both have samples readily available. However, they also have key differences including intrinsic growth pathway differences and response to immune modulation. My initial work focused on a retrospective study examining the feasibility of characterizing the tumor microenvironment utilizing the NanoString panels on archived paraffin tumor blocks in non-melanoma skin cancers. RNA was successfully isolated from primary CuSCC and basal cell carcinomas, and compared with respect to predetermined sets of genes characterizing different pathways involved in tumor, microenvironment and immune cell interactions in cancer (nCounter PanCancer, 2021). In addition to the nSolver Advanced Analysis software provided by Nanostring Technologies, another analysis software, Rosalind, was used to identify outliers, and the results were normalized to the expression of housekeeping genes provided by the nSolver software (nCounter Advanced Analysis, 2021).

We chose hedgehog (HH) signaling as a marker for a BCC genotype. This is because HH signaling has been found to be upregulated in sporadic BCC, but not in CuSCC (Walter et al., 2010; Lipson et al., 2017). A heat map portraying the HH signaling gene set showed a clear split between the gene expressions of CuSCC vs BCC (Figure 1). This is also supported by the HH signaling gene set's high undirected global significance score, which represents its extensive differential expression in BCC as compared to CuSCC (Supplemental Table 1). The results of this preliminary study confirms that the method of RNA extraction, as well as the quality of the samples, can produce accurate results from our sample collection.

Previous research has shown that BCC and CuSCC rely on different immune mechanisms for anti-tumor activity during the development of either cancer. For example, Walter and colleagues found that BCC expresses low levels of MHC-I molecules, which result in the lower numbers of infiltrating cytotoxic CD8+ T cells found in BCC in comparison to CuSCC (2010). Therefore, they conclude that immunosurveillance has a less prominent role during the development of BCC, making it relatively resistant to the adaptive immune system's anti-tumor activity that is seen in CuSCC. However, administering a Toll-like receptor 7 agonist immunotherapy, which consequently triggers the innate immune response, they found an upregulation of the MHC-I expression in BCC, which they interpreted as further supporting the role of the innate immunity instead of adaptive immunity for the anti-tumor activity in BCC patients (Walter et al., 2010). However, their observations could also be the tumor's way of evading an adaptive immune response, since antigen presentation in BCC could be overcome by innate stimulation, which would increase antigen presentation and allow for immune mediated tumor regression. Looking at immune activity in BCC lesions treated with Toll-like receptor 7 agonist immunotherapy at different points across a prolonged period of

time could help clarify the roles of innate vs. adaptive immunity in BCC progression and elimination.

CuSCC and BCC have the two highest mutational burdens in all cancers due to UV light exposure being the dominant risk factor in both cancers. The differential response between BCC and CuSCC to checkpoint therapy with PD1 pathway blockers provides an ideal experimental system to examine other factors determining T cell driven elimination of tumors (Sabbatino et al., 2018). One of those factors is the presence or absence of an IFN- γ signaling pathway. Tumors that respond to PD1 pathway blockade often have elevated gene expression linked to IFN- γ . Our results confirmed an increase in interferon signaling, cytotoxicity, and antigen presentation in CuSCC relative to BCC, highlighting the role of adaptive immunity in CuSCC. When comparing gene sets between CuSCC and BCC, the myeloid compartment, interferon signaling, cytotoxicity, and antigen presentation had the highest directed global significance score (Supplemental Table 1). Here, the directed global significance score measures the extent to which the genes in this set are up or downregulated, instead of measuring the overall differential expression in the global significance score. The gene sets most up-regulated in CuSCC compared to BCC all fall under the panel's key immuno-oncology signature of anti-tumor immune activity and tumor immunogenicity (nCounter PanCancer, 2021).

Having established and validated my methods in non-melanoma skin cancers, we then ran clinical samples from both immunocompetent and immunocompromised patients through the NanoStrings IO360 panel to compare gene expression profiles of precancerous skin malignancies leading up to CuSCC. We expect to show differential expression of genes

involved in TME and immune cell interactions (ie IFN pathway or TNF pathway) between these samples. Therefore, these findings can help us develop clinical prognostic gene expression profiles for CuSCC patients of any group. The profiles can also help find which patients would benefit from anti-PD-1 checkpoint blockade therapy or may require additional therapy modulations.

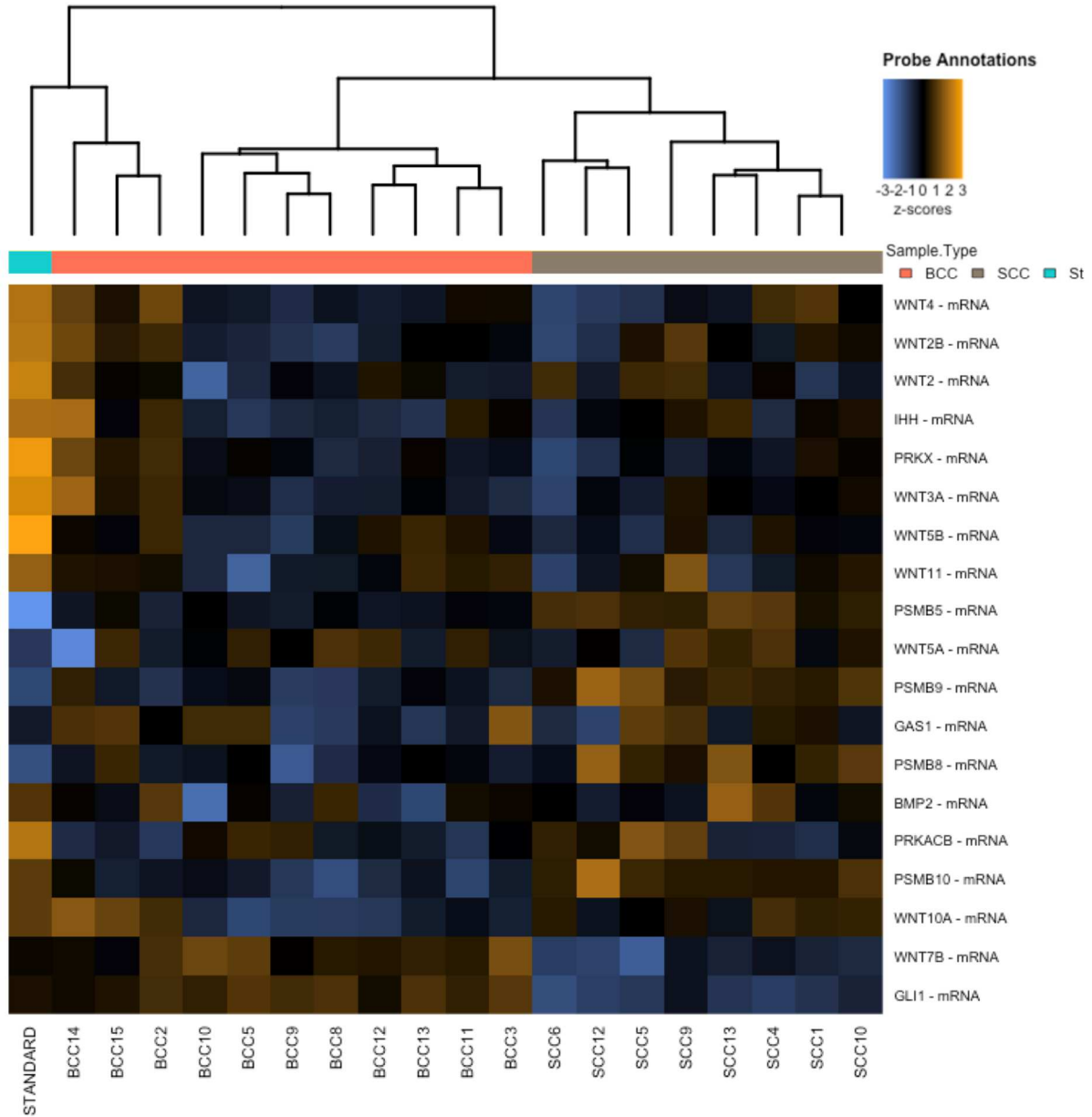


Figure 1. Heat map showing an upregulation of 19 hedgehog signaling pathway genes in basal cell carcinoma (BCC) samples that is not matched in the squamous cell carcinoma (SCC) samples. The phylogenetic tree at the top is generated by the NanoString Advanced Analysis unsupervised clustering algorithm to group similar samples within the data. The orange and grey bars under the BCC and SCC samples, respectively, indicate the distinct split between the gene expression signatures of the BCC vs SCC. Columns represent individual patients. Rows represent the specific genes involved in a hedgehog signaling gene expression profile, as set by the NanoString analysis software. The data is plotted by z-score on a normal distribution curve. In the probe annotations gradient scale, yellow indicates a high expression of the gene, blue indicates low expression.

3. Methods

3.1 Sample Collection and Processing:

Patients were identified from cases in the UCSD Dermatopathology Laboratory Information System, and samples were retrieved from the storage facility. Identified patients were non-organ transplant recipients with adequate samples for each of the following histologic groups: normal skin, actinic keratosis, actinic keratosis with follicular extension, hyperkeratotic actinic keratosis, squamous cell in situ, superficially invasive squamous cell carcinoma, crateriform squamous cell carcinoma, high risk squamous cell carcinoma, and moderately differentiated squamous cell carcinoma; as well as organ transplant recipients with adequate samples for each of the following histologic groups: normal skin, actinic keratosis, hyperkeratotic actinic keratosis, squamous cell in situ, superficially invasive squamous cell carcinoma, crateriform squamous cell carcinoma, high risk squamous cell carcinoma, and moderately differentiated squamous cell carcinoma. Patient charts were reviewed using the EPIC electronic medical record. Total RNA was isolated from four 5-20 μ m-thick FFPE sections of tumors per sample using the Qiagen RNeasy FFPE Kit following the manufacturer's protocols (Cat. No./ ID: 73504). The protocol produced 20ul of RNA in RNase free water, and the amount and quality of RNA per sample was confirmed using the NanoDrop ND1000 spectrophotometer, as well as the Qubit 4 Fluorometer (ThermoFisher Scientific). Gene expression analysis was conducted on the NanoString nCounter Sprint Profiler using the PanCancer Human IO360 Gene Expression Panel (NanoString Technologies). This panel includes probes for 770 different genes involved in tumor, microenvironment and immune cell interactions in cancer. These genes represent 13 different biological processes, as well as a tumor inflammation signature including 18 genes associated with response to the PD-1/PD-L1 immune checkpoint blockade therapy.

Analysis through the nSolver Advanced Analysis software provides customized normalization against either standard or chosen housekeeping genes, as well as differential expression to show gene expression changes in relation to experimental factors, cell profiling analysis to ratios of immune cell type markers in response to different variables, pathway clustering, RNA vs. protein level expression to differentiate transcriptional vs. translational responses, and a tumor inflammation score for each sample to distinguish inflamed vs. non-inflamed tumors. Using the normalized data processed and exported from the nSolver software, the ROSALIND platform is used for additional quality control to eliminate outlier samples with low imaging quality, binding density or limit of detection.

This study was approved by HRPP protocol # 190816 “Immunologic Characterization of Skin Cancers”.

3.2 NanoString nSolver Basic Analysis:

All samples were included in a preliminary analysis following the nSolver 4.0 Analysis Software User Manual. Annotations for each sample were added based on sample type. In the Positive Control Normalization, normalization factors below an average count of 100 were removed (POS_F). In the CodeSet Content Normalization, housekeeping genes with low count expression levels (under 100 count) were excluded from housekeeping normalization. Outlier housekeeping genes with much higher % Coefficient of Variation were also excluded from housekeeping normalization.

The Ratio Data Table from the first Basic Analysis was used to view the p-value, based on a t-test performed on groups of annotated samples, of the housekeeping genes in order to

eliminate any housekeeping genes that are significantly different expression levels across samples. Since there were many housekeeping genes with significantly different expression levels when comparing all sample types in pairwise ratios, the Basic Analysis was re-performed in two groups. In order to keep a more conservative approach to removing housekeeping genes, the samples were first divided into a non-transplant and an organ transplant group, then following the steps of the first Basic Analysis.

The Ratio Data Tables from the second Basic Analyses of both the non-transplant and organ transplant groups were then used to eliminate any housekeeping genes with significantly different expression levels across the samples of each group separately. For the non-transplant group, housekeeping genes TMUB2, STK11P, POLR2A, NRDE2, DNAJC14, TLK2, MRPL19, and SDHA were removed to perform a third Basic Analysis. For the organ transplant group, housekeeping genes GUSB, NRDE2, STK11P, TBP, TMUB2, SDHA, TLK2, PSMC4, ABCF1, PUM1, and ERCC3 were removed to also perform a third Basic Analysis. RCC files of the normalized data from the third Basic Analyses of both groups were imputed into the Rosalind platform for further quality control.

3.3 ROSALIND Analysis:

After performing the ROSALIND Analysis following the ROSALIND Quick Start Guide, visualization of the multidimensional scaling plot showed most non-transplant samples clustered together, and most organ transplant samples clustered together, except for a few outliers. Those samples were NTHigh4, NTMOD3, NTHAK3, and NTCRAT2 in the non-transplant group and OTAK5, OTAK2, OTCRAT3, and OTSUP3 in the organ transplant group. Those samples were considered outliers and excluded from the following Advanced Analysis.

3.4 NanoString nSolver Advanced Analysis:

Samples were chosen in pairwise comparisons (normal skin vs. actinic keratosis, actinic keratosis vs. squamous cell in situ, squamous cell in situ vs. invasive squamous cell carcinoma, for both non-transplant and organ transplant samples) and additional pairwise comparisons (normal skin vs. squamous cell in situ and normal skin vs. invasive squamous cell carcinoma for both non-transplant and organ transplant samples) were done in order to detect patterns that may be difficult to notice in the gradual comparisons between normal skin and actinic keratosis

3.5 Signature Score Analysis:

After housekeeping gene normalization, log₁₀ was applied to the raw expression data from the final round of basic analysis in the genes making up each of these following signature scores modified by Salas-Benito and colleagues (2021): IFN- γ signature (CXCL10, CXCL9, HLA-DRA, IDO1, IFNG, STAT1); modified expanded immune signature (CCL5, CD2, CD3D, CD3E, CXCL10, CXCL13, CXCR6, GZMB, GZMK, HLA-DRA, HLA-E, IDO1, IL2RG, LAG3, STAT1); and modified T-cell inflamed signature (CCL5, CD27, CD274, CD276, CD8A, CMKLR1, CXCL9, CXCR6, HLA- 7 DQA1, HLA-E, IDO1, LAG3, PDCD1LG2, PSMB10, STAT1, TIGIT). The signature scores were then calculated by averaging the log₁₀ expression of those genes in each of our samples, then taking the average score of all our samples in each sample type (non-transplant normal skin, non-transplant actinic keratosis, non-transplant squamous cell in situ, non-transplant invasive squamous cell carcinoma, organ transplant normal skin, organ transplant actinic keratosis, organ transplant squamous cell in situ, and organ transplant invasive squamous cell carcinoma) in order to create a signature score for each of the sample types.

4. Results

4.1 Non-Transplant Normal Skin (n=6) vs. Non-Transplant Actinic Keratosis (n=14)

In the non transplant group, there is no significant differentially expressed genes when comparing normal skin to actinic keratosis (NTNS vs. NTAK). For the other comparisons, the significant differentially expressed genes were first noted in the pathways with the highest global significance scores, which are calculated as the mean squared t-statistic for differential expression of genes in a pathway. Other significant differentially expressed genes were also deemed important if they play a role in multiple different pathways or have been of particular interest in previous literature.

4.2 Non-Transplant Actinic Keratosis (n=14) vs. Non-Transplant Squamous Cell In-Situ (n=7)

When comparing actinic keratosis to squamous cell in situ in non transplant patients (NTAK vs. NTIS), the pathways with the highest global significance scores are epigenetic regulation, cell proliferation, and metabolic stress (Table 1). EZH2 and NFKB1 are both upregulated in squamous cell in situ metabolic stress pathway, compared to actinic keratosis. NFKB1 also plays a role in multiple other pathways, however only cytokine and chemokine signaling, MAPK, and PI3K-Akt pathways have another significant differentially expressed gene in addition to the NFKB1 upregulation (Table 1). For example, MAPK have both NFKB1 and NGFR as significant differentially expressed genes, and even though there are no studies on the role of NGFR in squamous cell carcinoma, NGFR is considered a driver of melanoma, another type of invasive skin

cancer (Boshuizen et al., 2020). EZH2 upregulation also plays a role in the epigenetic regulation pathway, along with HELLS upregulation in squamous cell in situ compared to actinic keratosis. Three genes are significantly upregulated in the cell proliferation pathway of squamous cell in situ compared to actinic keratosis; ANLN, CDC25C, and KIF2C (Table 1). Cell proliferation has the greatest increase in pathway score from actinic keratosis to squamous cell in situ, which corresponds to an increased expression in a majority of the pathway's genes (Supplemental Fig. 1). Interestingly, NOTCH2 isn't significantly differentially expressed comparing actinic keratosis to squamous cell in situ (Table 1), unlike previous studies which have found NOTCH1/2/4 among the top three recurrently altered genes in CuSCC (Li et al., 2015). None of the significant differentially expressed genes coinciding with either the 6 gene IFN- γ signature or the 18 gene expanded immune signature predicting response to PD1 pathway blockade are observed.

4.3 Non-Transplant Squamous Cell In-Situ (n=7) vs. Non-Transplant Invasive Squamous Cell Carcinoma (n=26)

No genes are significantly differentially expressed between squamous cell in situ and invasive squamous cell carcinoma in non-transplant patients (NTIS vs. NTInv).

4.4 Non-Transplant Normal Skin (n=6) vs. Non-Transplant Squamous Cell In-Situ (n=7)

In order to visualize gene expression changes that may have not been apparent with the stepwise comparisons, we compared the squamous cell in situ samples to normal skin in non-transplant patients (NTNS vs. NTIS). In this comparison, the pathways with

the highest global significance scores are epigenetic regulation, autophagy, cell proliferation, and metabolic stress (Table 2). H2FAX is upregulated in the epigenetic regulation, cell proliferation, and metabolic stress pathways; while also playing a role in DNA damage repair; and BNIP3 is downregulated in the epigenetic regulation and autophagy pathways. Another gene upregulated in the autophagy pathway is PIK3CD, and plays a role in multiple other pathways such as cytokine and chemokine signaling, hypoxia, immune cell adhesion and migration, MAPK, and the PI3K-Akt pathways (Table 2). NRAS is also upregulated in both the autophagy and metabolic stress pathways, as well as plays a role in the cytokine and chemokine signaling, MAPK, and PI3K-Akt pathways. Other genes involved in the metabolic stress pathway are VHL, PFKM, and NBN (Table 2). However, no significant differentially expressed genes in this comparison coincide with either the IFN- γ or expanded immune signature.

4.5 Non-Transplant Normal Skin (n=6) vs. Non-Transplant Invasive Squamous Cell Carcinoma (n=26)

Finally, another method to compare the gene expression signature of squamous cell in situ and invasive squamous cell carcinoma was to compare both types against normal skin in non-transplant patients. When comparing invasive squamous cell carcinoma to normal skin (NTNS vs. NTInv), the pathways with the highest global significance scores are matrix remodeling and metastasis, metabolic stress, autophagy, and apoptosis (Table 3). LAMC2, LAMB3, MMP1, ITGA6, and ICAM1 are upregulated in the invasive squamous cell carcinoma matrix remodeling and metastasis pathway, compared to normal skin, but these genes also play roles in the PI3K-Akt pathway,

myeloid compartment pathway, and immune adhesion pathway. The upregulated genes in the metabolic stress pathway were PIK3CD, HIF1A, IL1A, MET, and PKM, some of which also play a role in the PI3K-Akt pathway (Table 3). PIK3CD and HIF-1A are also upregulated for the autophagy pathway, and for the apoptosis pathway, BAX is the only significant differentially expressed gene (Table 3). Overall, the matrix remodeling and metastasis, the metabolic stress, the cell proliferation, and the cytotoxicity pathways have the greatest increase in pathway score, in addition to the high global significance scores of the matrix remodeling and metastasis and the metabolic stress pathways, from normal skin to invasive squamous cell carcinoma (Supplemental Fig. 2), which means the majority of the pathway's genes also increased. Although not included in the pathways with the highest global significance scores, CXCL13, the only gene coinciding with the 18 gene expanded immune signature, is upregulated in the lymphoid compartment and the cytokine and chemokine signaling pathways (Table 3). Other genes from the expanded immune signature are upregulated in invasive squamous cell carcinoma compared to normal skin, however, they aren't statistically significant.

Therefore, we divided the non-transplant invasive squamous cell group into the samples we know are the most poorly differentiated subgroups; moderately differentiated and high-risk (poorly differentiated) squamous cell carcinoma. When comparing the moderately and poorly differentiated squamous cell carcinoma to the normal skin (NTNS vs. NTMod NTHigh), many more genes from the 18 gene expanded immune signature are significantly differentially expressed. In this case, LAG3, CXCL13, CXCL5, IDO1, and CCL5 are all upregulated in moderately and poorly differentiated squamous cell carcinoma, in either one of the costimulatory signaling, cytokine and chemokine

signaling, lymphoid compartment, and myeloid compartment pathways, compared to normal skin (Table 4). CXCL10 is also upregulated in this comparison, although it isn't statistically significant. This comparison shows a more visible change in immune signature from normal skin to invasive squamous cell carcinoma, although the gradual stepwise change is not visible in previous comparisons to distinguish at what stage did the switch from no immune signature to immune infiltration happen, and what could be the driver of that switch.

4.6 Organ Transplant Normal Skin (n=2) vs. Organ Transplant Actinic Keratosis (n=12)

Unlike the normal skin to actinic keratosis in non-transplant patients, there are, in fact, significant differentially expressed genes in the normal skin to actinic keratosis comparison in organ transplant patients (OTNS vs OTAK). For this comparison, the pathways with the highest global significance scores are matrix remodeling and metastasis, metabolic stress, autophagy, and angiogenesis (Table 5). In the angiogenesis pathway, both FGFR1 and FGF18 are significantly differentially expressed, and both also play roles in the MAPK as well as the PI3K-Akt pathways. The significant differentially expressed gene in the autophagy pathway, PTEN, also plays a role in the PI3K-Akt pathway (Table 5). In addition to FGFR1 and PTEN, the metabolic stress pathway has other significant differentially expressed genes that also play a role in the PI3K-Akt pathway, such as EIF4EBP1 and CDKN1A, as well as genes that are involved in metabolic stress, such as TPI1 and RICTOR. For the matrix remodeling and metastasis pathway, the two genes that are significantly downregulated are NCAM1 and RELN

(Table 5). None of the significant differentially expressed genes in this comparison coincide with the IFN- γ signature or the expanded immune signature, however, a downregulation of NOTCH2 is observed, which reinforces findings in previous literature where NOTCH family members are estimated to be inactive in a quarter of their metastatic CuSCC samples (Li et al., 2015). Unfortunately, however, there are only two samples in the organ transplant normal skin group. This must be taken into consideration when analyzing these results since a sample size of two has very low statistical power, especially after adjusting for multiple comparison correction, and increases the probability of observing such results by chance. In other words, there might be more differentially expressed genes that we are unable to find in this comparison.

4.7 Organ Transplant Actinic Keratosis (n=12) vs. Organ Transplant Squamous Cell In-Situ (n=7)

Similar to the actinic keratosis and squamous cell in situ comparison in non-transplant patients, the actinic keratosis and squamous cell in situ comparison in organ transplant patients (OTAK vs. OTIS) has only one significant differentially expressed gene, RAD51, which only plays a role in the cell proliferation and the DNA damage repair pathways (Table 6). However, given that it is only one significant gene in either one of those comparisons, it may not be enough to determine if those pathways really play a role in the progression of cancer.

4.8 Organ Transplant Squamous Cell In-Situ (n=7) vs. Organ Transplant Invasive Squamous Cell Carcinoma (n=23)

When comparing squamous cell in situ to invasive squamous cell carcinoma in organ transplant patients (OTIS vs. OTInv), the pathways with the highest global significance scores are the myeloid compartment, MAPK, and matrix remodeling and metastasis pathways (Table 7). However, only one gene in each of those pathways is significantly differentially expressed: SIRPA, FAS, and LOXL2 respectively. Interestingly, the one gene that is significantly downregulated in the interferon pathway in this comparison is HLA-DRB5 (Table 7), coding for the same MHC cell surface receptor isotype as both the HLA-DRA in the IFN- γ signature and additionally the HLA-DRE genes in the expanded immune signature. This may point to a downregulation of immune infiltrate in the invasive squamous cell carcinoma of organ transplant recipients, since this MHC cell surface receptor would be found on dendritic cells, macrophages, B cells, helper T cells, and other immune cells that would normally recognize the tumor. Since there was a significant downregulation of HLA-DRB5, this would point to a measure of how deep the immune suppression is in organ transplant patients, which explains the 100-250 fold increased risk of CuSCC in immunosuppressed patients (Inman et al., 2018).

Interestingly however, when comparing squamous cell in situ to specifically the most poorly differentiated invasive squamous cell carcinoma subgroups in organ transplant recipients; moderately and poorly differentiated squamous cell carcinoma (OTIS vs. OTMod OTHigh), there are no significant differentially expressed genes in any pathway. Similarly, when comparing squamous cell in situ to the other two subgroups that make up invasive squamous cell carcinoma; superficial and crateriform invasive squamous cell carcinoma (OTIS vs. OTSUP OTCRAT), we notice the same lack of

significant differentially expressed genes; even the HLA-DRB5 that we previously related to an immune signature disappears here. However, the lack in differentially expressed genes in these two comparisons could also be due to cutting the sample size of the invasive squamous cell carcinoma patients in half when comparing to only OTMod and OTHigh or OTSUP and OTCRAT.

4.9 Organ Transplant Normal Skin (n=2) vs. Organ Transplant Squamous Cell In-Situ (n=7) and Organ Transplant Normal Skin (n=2) vs. Organ Transplant Invasive Squamous Cell Carcinoma (n=23)

Again, in order to visualize gene expression changes that may have not been apparent with the stepwise comparisons, we compared the squamous cell in situ samples to normal skin in organ transplant patients (OTNS vs. OTIS). In this comparison, the pathways with the highest global significance scores are the matrix remodeling and metastasis, interferon signaling, immune cell adhesion and migration, and angiogenesis pathways (Table 8). The downregulation of NCAM1 is responsible for the high global significance scores of the matrix remodeling and metastasis, interferon signaling, and immune cell adhesion and migration pathways, whereas the downregulation of FGR1 is responsible for the high global significance score of the angiogenesis pathway. FGR1 also plays a role in the MAPK, metabolic stress, and PI3K-Akt pathways, however, for all these pathways with the highest global significance scores, only one gene in each pathway is significantly differentially expressed (Table 8). In this comparison, just like the normal skin to actinic keratosis in organ transplant patients, there were only two samples of normal skin available to analyze, therefore the organ transplant normal skin

group didn't have enough statistical power, especially after a multiple comparison correction. However, we also performed a normal skin to invasive squamous cell carcinoma comparison in organ transplant patients (OTNS vs. OTInv), as well as normal skin to only moderately and poorly differentiated squamous cell carcinoma (OTNS vs. OTMod OTHigh), despite the low statistical power of the normal skin group and found no significant differentially expressed genes in any pathway of either comparison. These results confirmed the low sensitivity in our data when comparing against a group of only two samples (OTNS), since we expected a downregulation of genes in the interferon signature or expanded immune signature, as we saw in the squamous cell in situ to invasive squamous cell carcinoma comparison in organ transplant recipients.

5. Discussion

The transition from normal skin to cancer is a complex multistep event marked by both intrinsic metabolic pathway changes and extrinsic immune selection. Identifying these steps could be important in identifying prevention strategies and as predictors of response to therapy. I have applied the molecular characterization technique using Nanostring to determine when these steps occur and how they may relate to phenotypic changes marking cancer progression.

Previous research studying the genomic characterization of CuSCC identified recurring NOTCH family mutations as one of the most common events in CuSCC due to NOTCH's role in promoting cell differentiation (Cheng et al., 2014). The only instance of significant differential expression of a NOTCH family gene, NOTCH2, was in the comparison between normal skin and actinic keratosis in the organ transplant recipient samples (Table 5). In this comparison, NOTCH2 is downregulated in actinic keratosis as compared to normal skin which would corroborate previous studies that find loss of function mutations in NOTCH family genes (Wang et al., 2011). However, those genomic characterization studies were done on CuSCC on non-organ transplant recipients, and didn't mention actinic keratosis. So the downregulation of NOTCH2 we found could either signify that NOTCH loss of function mutations are a very early event in the formation of CuSCC, therefore it can be found in as early as actinic keratosis, or the result we found could be due to other factors unrelated to the formation of CuSCC, instead mostly due to the very low statistical power of our OTNS group, especially since the NOTCH2 downregulation wasn't found in any other comparison against OTNS, and wasn't seen in any of the non-transplant sample comparisons either.

Another gene that was found in a couple comparisons against normal skin samples in organ transplant recipients was FGFR1 (Table 5, Table 8), part of the FGFR family genes involved in cell differentiation and proliferation (Grose & Dickson, 2005). FGFR upregulation has been seen in multiple cancers, since its downstream pathways include the PI3K-AKT pathway, MAPK pathway, and MTOR pathway, all commonly found in cancer to suppress autophagy and inducing malignant cell proliferation (Khandelwal et al., 2019). Khandelwal and colleagues found increased FGFR2 phosphorylation with exposure to UVB when studying mouse skin samples (2019). They also found consistent overexpression of FGFR2 in all the CuSCC cell lines they tested, and when administering an FGFR inhibitor, its effect on the suppression of CuSCC was primarily through FGFR2 inhibition instead of FGFR1 (Khandelwal et al., 2019). However, our experiment saw a downregulation of FGFR1 in both actinic keratosis and squamous cell in situ in comparison to normal skin in organ transplant recipients (Table 5, Table 8). Therefore, it is again possible that this result is not due to the formation of CuSCC and instead due to the low statistical power of OTNS, or that in this case, FGFR1 actually works in opposition to the FGFR2 studied in Khandelwal and colleagues' samples, since Khandelwal and colleagues also recognized that previous studies have seen opposite roles to FGFR2 in skin cancer, both cancer promoting and suppressing (2019).

In a study of the role of NGFR in melanoma immune therapy resistance, Boshuizen and colleagues showed that not only does NGFR predict resistance to multiple immune therapies, but actually plays a causal role in T cell resistance and exclusion (2020). When comparing actinic keratosis to squamous cell in situ in non-transplant

patient samples, NGFR was unexpectedly downregulated in squamous cell in situ (Table 1). According to Boshuizen and colleagues, there are two subpopulations of melanoma cells that can express NGFR, a population of NGFR expressing cells that pre-exist in melanoma patients and is stably maintained in melanoma cell lines, largely irreversible, and a population of NGFR negative cells that after repeated exposure to T cells are able to escape recognition by differentiation and acquire the reversible expression of NGFR (2020). The downregulation of NGFR from actinic keratosis to squamous cell in situ seen in our data set would more likely match the subpopulation of NGFR expressing cells that pre-exist in the tumor (if we are to assume that CuSCC, like melanoma, contains that pre-existing subpopulation of cells), since the NGFR expression is seen in the early actinic keratosis event, and could point to the ability to reverse NGFR in that previously assumed irreversible subpopulation of NGFR expressing cells, since NGFR is downregulated in the later squamous cell in situ event. But again, this differential expression could be due to the small sample sizes and overall low statistical power of our study.

Epigenetic regulators also have been previously considered as a target for cancer therapy with different patient responses and varying success. Therefore, there may be a significance to differentially expressed genes in the epigenetic regulation pathway, more than just the nature of the mutations causing the cancer. For example, EZH2 has not only been seen to play a role in cell proliferation and metastasis through epithelial-mesenchymal transition, but in a study by Kryczek and colleagues in ovarian cancer, EZH2 was found to repress the tumor's production of chemokine CXCL9 and CXCL10, which was ultimately negatively associated with CD8 T cell infiltration of the tumor

(2016). Patient outcome was also negatively associated with EZH2 expression as Zingg and colleagues found that during anti-CTLA-4 and IL-2 therapies, the increase of T cells and TNF- α as a response to the therapy actually increased EZH2, which in turn decreased the tumor's antigen presentation allowing it to escape immune detection (2017). EZH2 was also found to recruit immune suppressing regulatory T cells to reduce inflammation (Yang et al., 2015). In our study, EZH2 was upregulated when comparing actinic keratosis to squamous cell in situ in non-transplant patient samples. This finding backs up the hypothesis that on the evolution from normal skin to invasive CuSCC, malignant cells must evade immune detection especially in immunocompetent patients who have not undergone organ transplant. EZH2 upregulation was therefore not found in any of the malignant organ transplant patient samples, probably since those tumors have already escaped immune recognition due to the immunocompromised state of those patients. Chromatin modulator inhibitors such as inhibiting EZH2 expression has been introduced as a therapeutic strategy, as well as in combination with chemotherapy, however, due to the tumor suppressive qualities of EZH2 as well, further investigation is required (Yang et al., 2015). HELLS is another gene in the epigenetic regulation pathway that is highly expressed in proliferating tissue, with the highest expression of HELLS in stem cells and expression decreases as the cells differentiate (Han et al., 2017). However, the role of HELLS in cancer development has not yet been identified since in some cancers, mutations have caused an increase in HELLS expressions while in others, HELLS expression is decreased (Robinson et al., 2019). In our experiment, HELLS was upregulated when comparing actinic keratosis to squamous cell in situ in non-transplant patient samples (Table 1). Similarly to HELLS, BNIP3 has been shown to be both a

tumor promoter, by promoting cell survival, and tumor suppressor, by inducing apoptosis (Gorbunova et al., 2020). Previous studies have found BNIP3 to be over expressed in many different cancers and at different points of the tumor's progression, so its exact role has not yet been described. For example, in gastric cancer, Sugita and colleagues found that lower levels of BNIP3 correlated with resistance to therapy and poor prognosis (2011). However, Vara-Pérez and colleagues' study in melanoma found that increased levels of BNIP3 correlated with poorer prognosis due to BNIP3's role upstream of the tumor promoting HIF-1a glycolysis pathway, allowing the melanoma cells to continue to grow (2021). Since our results found BNIP3 downregulated in normal skin vs squamous cell in situ in non-transplant patient samples (Table 1), but also found HIF-1a upregulated in normal skin to invasive skin in non-transplant patient samples (Table 3), it is difficult to identify both BNIP3 and HIF-1a's role in determining patient prognosis, as well as their role in the formation of invasive CuSCC.

To address our initial question of how CuSCC escapes immune recognition differently in immunocompromised vs. immunocompetent patients, we specifically examined the immunologic evolution of CuSCC. Since previous literature have showed that IFN- γ is a driver of PD-L1 expression in cancer, as well as that T cell infiltration into the tumor microenvironment (TME) may improve response to anti-PD-1 therapies, we focused on the genes described in Ayers and colleagues as part of the 6 gene IFN- γ signature and 18 gene expanded immune signature (2017). The only comparison that showed multiple differentially expressed genes in either of those signatures was the comparison moderately and poorly differentiated squamous cell carcinoma to normal skin in non-transplant patients. LAG3, CXCL13, CXCL5, IDO1, and CCL5 were all

significantly upregulated in moderately and poorly differentiated squamous cell carcinoma, as well as CXCL10, but with a non-significant pvalue higher than 0.05. According to the research by Ayers and colleagues, these genes are directly linked to IFN- γ expression in order to predict responders and non-responders to anti-PD-1 therapy in melanoma and other cancers, therefore the upregulation of these genes in our samples of moderately and poorly differentiated squamous cell carcinoma in non-transplant patients identify a population that could respond to anti-PD-1. We would expect precancerous areas of actinic keratosis and squamous cell in situ disease to not respond to PD-1 pathway blockade as they lack this signature. Agents that induce this signature could be rationally partnered with PD-1 pathway blockade in early diseases states or in cancers that lack this signature (ie basal cell cancers).

In contrast, the other comparison that may have a differentially expressed gene related to the IFN- γ or expanded immune signature is squamous cell in situ to invasive squamous cell carcinoma in organ transplant patients (Table 6). In the case of samples from organ transplant patients, HLA-DRB5 is significantly downregulated in invasive squamous cell carcinoma, showing at least one gene that may point to a decrease in the IFN- γ or expanded immune signature in the invasive cancer compared to a precancerous lesion (Table 6). The increase in IFN- γ or expanded immune signature in the invasive CuSCC in non-transplant patients, and the possible decrease in the IFN- γ or expanded immune signature in the invasive CuSCC in transplant patients supports the hypothesis that formation of invasive CuSCC is dependent on different pathways to escape immune recognition in an immunosuppressed vs. an immunocompetent environment, since this difference in the IFN- γ or expanded immune signature may signify the immune system

recognizing the invasive cancer in the non-transplant patients, but not recognizing it in the immunosuppressed organ transplant patients. As invasive cancers in transplant patients occur in the most immunosuppressed group, monitoring the immune signature of the skin could help risk stratify patients as high or low risk of progressing to cancer.

In order to evaluate a more quantitative analysis of the IFN- γ and expanded immune properties of our samples, we calculated 3 different signature scores as described in Salas-Benito and colleagues for each sample type (2021). The signatures we calculated were the IFN- γ signature (CXCL10, CXCL9, HLA-DRA, IDO1, IFNG, STAT1), modified expanded immune signature (CCL5, CD2, CD3D, CD3E, CXCL10, CXCL13, CXCR6, GZMB, GZMK, HLA-DRA, HLA-E, IDO1, IL2RG, LAG3, STAT1), and modified T-cell inflamed signature (CCL5, CD27, CD274, CD276, CD8A, CMKLR1, CXCL9, CXCR6, HLA-DQA1, HLA-E, IDO1, LAG3, PDCD1LG2, PSMB10, STAT1, TIGIT). There was very little variation in the three previously mentioned significance scores between any of the comparisons in both organ transplant and non-transplant patient samples. These calculations confirm the minimal or even lack of significantly differentially expressed genes between the comparisons previously described, and further brings into question the significance of the few genes that we did find upregulated when comparing the moderately differentiated and high risk (poorly differentiated) squamous cell carcinoma to the normal skin in the non-transplant patient samples (the scores considered all invasive, not just moderately differentiated and high risk).

These results come with many limitations expected when using a small number of clinical samples, as well as using a panel with limited number of genes instead of whole genome sequencing. Another limitation is in the normalization and analysis platform

NanoString provides, since some of the provided housekeeping genes were not stable enough across samples to be normalized against, as well as additional rounds of normalization that were decided on after inputting the data into the Rosalind platform and trying different runs of the advanced analysis. Therefore, changing the order, frequency, or types of normalizations during the NanoString basic analysis can change the significance of the outliers found and removed from the study, and with the small number and heterogeneous populations of samples, change the significance of the differentially expressed genes in those samples. Also, the NanoString bioinformatics advanced analysis, although user-friendly, lends itself well to pairwise comparisons, but significance scores and p-values cannot be weighed across pairwise comparisons. Therefore, studies like this one trying to find a gradual evolution throughout a cancer's progression may not notice patterns as easily as by comparing all the different sample types together. This is where the IFN- γ signature, modified expanded immune signature, and modified T-cell inflamed signature scores come in to quantitatively normalize significance across different comparisons.

While NanoString has proved in many previous studies to be highly reproducible, especially with RNA isolated from FFPE samples, and definitely provides ease of use for preliminary studies focusing on particular pathways of interest, one of its limitations for studying immune response is tissue heterogeneity. RNA analyzed by the IO360 panel considers the entire tumor as a whole, whereas in reality, variable amounts of different immune cells are located in different parts of the tumor microenvironment (tumor cells and surrounding stromal cells). For that, more expensive and complicated techniques are used for gene expression profiling, such as DNA microarrays or RNAseq, but these

approaches require rarer fresh tissue, are not as resilient to more degraded samples available in FFPE tissue, and may not be available for laboratories with more limited resources.

Gene expression profiling has been used in clinical settings for prognostic and predictive indications in many types of cancers including melanomas (Armanious et al., 2020) The use of the NanoString panel makes it easier and more cost effective to study which types of cells are infiltrating the tumor through a genomic signature approach instead as an adjunct assay for cancer prognoses and diagnoses (Armanious et al., 2020). And finally, the newer NanoString GeoMX Digital Spacial Profile platform can now provide specific region of interest selection to view the profiling data in order to solve the limitations that come with the tissue heterogeneity in previous panels, and can be used to find target genes in any region of the tumor microenvironment (GeoMx DSP, 2021)

Overall, our study did not show any similarities between the significantly differentially expressed genes in the evolution from normal skin to invasive CuSCC in the non-transplant patient samples compared to the organ transplant patient samples, signifying the likelihood that the formation of an invasive cancer was dependent on different pathways to escape immune recognition in non-transplant patients vs. organ transplant patients as hypothesized. One explanation is that immunocompetent patients need to undergo immune evolution in order for the tumor to escape immune recognition, with the aid of epigenetic modifications, while organ transplant patients do not have the same pressure to undergo immune evolution since their immune system is already suppressed and the tumor can already escape recognition. As we've shown in our comparison between squamous cell in-situ and invasive squamous cell carcinoma in

organ transplant recipients, an important factor in organ transplant patients' lack of immune recognition is their significant downregulation of MHC class II, and therefore downregulation of immune infiltrates. However, since the normal, actinic keratosis, in situ and invasive samples were obtained from different patients, the patient variability, given the small sample size, could have precluded from seeing the evolution of the genetic profile of the same patient through the progression of skin cancer. Future experiments with a much larger cohort and ideally a longitudinal study following each patient separately through the evolution of their CuSCC would allow us to specifically watch the genetic expression changes over time on a patient by patient basis to hopefully see a clearer pattern of immunologic evolution in non-melanoma skin cancer development.

6. Tables

Table 1: Table of significantly differentially expressed genes and the pathways in which they are involved when comparing actinic keratosis to squamous cell in situ in non-transplant patients. Pathways with the highest global significance scores are indicated with *. Genes highlighted in blue are upregulated with $pvalue < 0.05$. Genes highlighted in green are downregulated with $pvalue < 0.05$.

Comparison					
All NTAK vs. NTIS					
Angiogenesis		EZH2			
Antigen Presentation		KIF2C			
Apoptosis					
Autophagy					
Cell Proliferation	*	KIF2C	CDC25C	ANLN	
Costimulatory Signaling		NFKB1			
Cytokine and Chemokine Signaling		NFKB1	CCL18		
Cytotoxicity					
DNA Damage Repair					
Epigenetic Regulation	*	HELLS	EZH2		
Hedgehog Signaling					
Hypoxia		NFKB1			
Immune Cell Adhesion and Migration					
Interferon Signaling					
JAK-STAT Signaling					
Lymphoid Compartment					
MAPK		NFKB1	NGFR		
Matrix Remodeling and Metastasis					
Metabolic Stress	*	NFKB1	EZH2		
Myeloid Compartment					
NF-kappaB Signaling		NFKB1			
Notch Signaling					
PI3K-Akt		NFKB1	NGFR		
TGF-beta Signaling					
Wnt Signaling			SFRP1		

Table 2: Table of significantly differentially expressed genes and the pathways in which they are involved when comparing normal skin to squamous cell in situ in non-transplant patients. Pathways with the highest global significance scores are indicated with *. Genes highlighted in yellow are upregulated with $pvalue < 0.01$. Genes highlighted in blue are upregulated with $pvalue < 0.05$. Genes highlighted in green are downregulated with $pvalue < 0.05$.

Comparison	Angiogenesis	Antigen Presentation	Apoptosis	Autophagy	Cell Proliferation	Costimulatory Signaling	Cytokine and Chemokine Signaling	Cytotoxicity	DNA Damage Repair	Epigenetic Regulation	Hedgehog Signaling	Hypoxia	Immune Cell Adhesion and Migration	Interferon Signaling	JAK-STAT Signaling	Lymphoid Compartment	MAPK	Matrix Remodeling and Metastasis	Metabolic Stress	Myeloid Compartment	NF-kappaB Signaling	Notch Signaling	PI3K-Akt	TGF-beta Signaling	Wnt Signaling	
NTNS vs. NTIS		VHL	FADD	NRAS	H2AFX	LY9	NRAS		H2AFX	*		VHL	CDH5		PIK3CD	LY9	NRAS		*	NRAS				NRAS		SFRP1
		MRC1		BNIP3	NBN		CCL18		NBN			PIK3CD	PIK3CD				PIK3CD		H2AFX	H2AFX			PIK3CD			
																			VHL							

Table 3: Table of significantly differentially expressed genes and the pathways in which they are involved when comparing normal skin to invasive squamous cell carcinoma in non-transplant patients. Pathways with the highest global significance scores are indicated with *. Genes highlighted in yellow are upregulated with pvalue<0.01. Genes highlighted in pink are downregulated with pvalue<0.01. Genes highlighted in blue are upregulated with pvalue<0.05.

Comparison	Angiogenesis	Antigen Presentation	Apoptosis	Autophagy	Cell Proliferation	Costimulatory Signaling	Cytokine and Chemokine Signaling	Cytotoxicity	DNA Damage Repair	Epigenetic Regulation	Hedgehog Signaling	Hypoxia	Immune Cell Adhesion and Migration	Interferon Signaling	JAK-STAT Signaling	Lymphoid Compartment	MAPK	Matrix Remodeling and Metastasis	Metabolic Stress	Myeloid Compartment	NF-kappab Signaling	Notch Signaling	PI3K-Akt	TGF-beta Signaling	Wnt Signaling
NTNS vs. all NTInv			*	*															*	*					
			BAX	PIK3CD	RBL2		PIK3CD	ISG15	ISG15			PIK3CD	PIK3CD	ISG15	PIK3CD	CXCL13	PIK3CD	LAMC2	PIK3CD			HIF1A	LAMC2	RBL2	
			TNFRSF10B	HIF1A			CXCL13					HIF1A	ITGA6	ICAM1		ISG15	IL1A	LAMB3	HIF1A				LAMB3	INHBA	
							IL1A						ICAM1				MET	MMP1	IL1A				RBL2		
																		ITGA6	MET				PIK3CD		
																		ICAM1					ITGA6		
																							MET		

Table 4: Table of significantly differentially expressed genes and the pathways in which they are involved when comparing normal skin to moderately differentiated and high risk squamous cell carcinoma in non-transplant patients. Pathways with the highest global significance scores are indicated with *. Genes highlighted in yellow are upregulated with pvalue<0.01. Genes highlighted in blue are upregulated with pvalue<0.05. Genes highlighted in green are downregulated with pvalue<0.05.

Comparison	Angiogenesis	Antigen Presentation	Apoptosis	Autophagy	Cell Proliferation	Costimulatory Signaling	Cytokine and Chemokine Signaling	Cytotoxicity	DNA Damage Repair	Epigenetic Regulation	Hedgehog Signaling	Hypoxia	Immune Cell Adhesion and Migration	Intestine Signaling	JAK-STAT Signaling	Lymphoid C compartment	MAPK	Matrix Remodeling and Metastasis	Metabolic Stress	Myeloid Compartment	NF-kappaB Signaling	Notch Signaling	PI3K-Akt	TGF-beta Signaling	Wnt Signaling
NTNS vs. NTMod	FGFR1	MRC1	BAX	HIF1A	CCNA1	SPP1	IL1B	ISG15	ISG15		PSMB9	HIF1A	PK3CD	ISG15	PK3CD	ISG15	MET	LAMC2	MET	LAMB3	PSMB9	HIF1A	LAMC2	INHBA	
NTHigh	MMP9	PSMB9	CD14	PK3CD	NBN	LAG3	CXCL5	IL1RA	CCNA1			PK3CD	PK3CD	IFIT3	IL1RA	CXCL13	IL1B	SPP1	MET	IL1B		DTXL	MET		
		TAP1	FADD		RBL2	CD80	PK3CD	IL2RB2	NBN			PK3CD	ICAM1	ICAM1	IL24	LAG3	KIT	LAMB3	KIT	IL1B	SERPINA1	DTXL	SPP1	TOFB3	
		UBE2C	BIRC5		CCNA1	PSMB9	PK3CD	GNLY				LDHA	PVR	GBP1	IL2RB2	IL2RB2	PK3CD	PLOD2	PK3CD	SIC1A1			LAMB3	RBL2	
		HLA-F			CEP55		CXCL12	IFIT3				CDH5	ITAG6	IFIT2	GNLY	IL1A	ICAM1	ITAG6	CXCL8	CXCL5			KIT		
					BIRC5		CXCL18	PRF1				ITAG6	CD80	HLA-F	PRF1	IL1A	ICAM1	ITAG6	IL1A	CXCL12			PK3CD		
					PSMB9		IL1RA	IFIT2				MMP9	MMP9	HLA-F	PVR	IL1A	ICAM1	ITAG6	IL1A	CXCL12			ITAG6		
					UBE2C		IL1A	IFIT2				HLA-F	HLA-F		SLAMF7	CD14	ICAM1	ITAG6	IL1A	CXCL12			TLR2		
							CCL3L1								IDO1	CD14	ICAM1	ITAG6	IL1A	CXCL12			RBL2		
							CCL4								CD9A	CD9A	ICAM1	ITAG6	IL1A	CXCL12			FGFR1		
							IL2RB2								CD9A	CD9A	ICAM1	ITAG6	IL1A	CXCL12					
															CD9A	CD9A	ICAM1	ITAG6	IL1A	CXCL12					
															CD9A	CD9A	ICAM1	ITAG6	IL1A	CXCL12					
															CD9A	CD9A	ICAM1	ITAG6	IL1A	CXCL12					
															CD9A	CD9A	ICAM1	ITAG6	IL1A	CXCL12					
															CD9A	CD9A	ICAM1	ITAG6	IL1A	CXCL12					
															CD9A	CD9A	ICAM1	ITAG6	IL1A	CXCL12					
															CD9A	CD9A	ICAM1	ITAG6	IL1A	CXCL12					
															CD9A	CD9A	ICAM1	ITAG6	IL1A	CXCL12					
															CD9A	CD9A	ICAM1	ITAG6	IL1A	CXCL12					
															CD9A	CD9A	ICAM1	ITAG6	IL1A	CXCL12					
															CD9A	CD9A	ICAM1	ITAG6	IL1A	CXCL12					
															CD9A	CD9A	ICAM1	ITAG6	IL1A	CXCL12					
															CD9A	CD9A	ICAM1	ITAG6	IL1A	CXCL12					
															CD9A	CD9A	ICAM1	ITAG6	IL1A	CXCL12					
															CD9A	CD9A	ICAM1	ITAG6	IL1A	CXCL12					
															CD9A	CD9A	ICAM1	ITAG6	IL1A	CXCL12					
															CD9A	CD9A	ICAM1	ITAG6	IL1A	CXCL12					
															CD9A	CD9A	ICAM1	ITAG6	IL1A	CXCL12					
															CD9A	CD9A	ICAM1	ITAG6	IL1A	CXCL12					
															CD9A	CD9A	ICAM1	ITAG6	IL1A	CXCL12					
															CD9A	CD9A	ICAM1	ITAG6	IL1A	CXCL12					
															CD9A	CD9A	ICAM1	ITAG6	IL1A	CXCL12					
															CD9A	CD9A	ICAM1	ITAG6	IL1A	CXCL12					
															CD9A	CD9A	ICAM1	ITAG6	IL1A	CXCL12					
															CD9A	CD9A	ICAM1	ITAG6	IL1A	CXCL12					
															CD9A	CD9A	ICAM1	ITAG6	IL1A	CXCL12					
															CD9A	CD9A	ICAM1	ITAG6	IL1A	CXCL12					
															CD9A	CD9A	ICAM1	ITAG6	IL1A	CXCL12					
															CD9A	CD9A	ICAM1	ITAG6	IL1A	CXCL12					
															CD9A	CD9A	ICAM1	ITAG6	IL1A	CXCL12					
															CD9A	CD9A	ICAM1	ITAG6	IL1A	CXCL12					
															CD9A	CD9A	ICAM1	ITAG6	IL1A	CXCL12					
															CD9A	CD9A	ICAM1	ITAG6	IL1A	CXCL12					
															CD9A	CD9A	ICAM1	ITAG6	IL1A	CXCL12					
															CD9A	CD9A	ICAM1	ITAG6	IL1A	CXCL12					
															CD9A	CD9A	ICAM1	ITAG6	IL1A	CXCL12					
															CD9A	CD9A	ICAM1	ITAG6	IL1A	CXCL12					
															CD9A	CD9A	ICAM1	ITAG6	IL1A	CXCL12					
															CD9A	CD9A	ICAM1	ITAG6	IL1A	CXCL12					
															CD9A	CD9A	ICAM1	ITAG6	IL1A	CXCL12					
															CD9A	CD9A	ICAM1	ITAG6	IL1A	CXCL12					
															CD9A	CD9A	ICAM1	ITAG6	IL1A	CXCL12					
															CD9A	CD9A	ICAM1	ITAG6	IL1A	CXCL12					
															CD9A	CD9A	ICAM1	ITAG6	IL1A	CXCL12					
															CD9A	CD9A	ICAM1	ITAG6	IL1A	CXCL12					
															CD9A	CD9A	ICAM1	ITAG6	IL1A	CXCL12					
															CD9A	CD9A	ICAM1	ITAG6	IL1A	CXCL12					
															CD9A	CD9A	ICAM1	ITAG6	IL1A	CXCL12					
															CD9A	CD9A	ICAM1	ITAG6	IL1A	CXCL12					
															CD9A	CD9A	ICAM1	ITAG6	IL1A	CXCL12					
															CD9A	CD9A	ICAM1	ITAG6	IL1A	CXCL12					
															CD9A	CD9A	ICAM1	ITAG6	IL1A	CXCL12					
															CD9A	CD9A	ICAM1	ITAG6	IL1A	CXCL12					
															CD9A	CD9A	ICAM1	ITAG6	IL1A	CXCL12					
															CD9A	CD9A	ICAM1	ITAG6	IL1A	CXCL12					
															CD9A	CD9A	ICAM1	ITAG6	IL1A	CXCL12					
															CD9A	CD9A	ICAM1	ITAG6	IL1A	CXCL12					
															CD9A	CD9A	ICAM1	ITAG6	IL1A	CXCL12					
															CD9A	CD9A	ICAM1	ITAG6	IL1A	CXCL12					
															CD9A	CD9A	ICAM1	ITAG6	IL1A	CXCL12					
															CD9A	CD9A	ICAM1	ITAG6	IL1A	CXCL12					
															CD9A	CD9A	ICAM1	ITAG6	IL1A	CXCL12					
															CD9A	CD9A	ICAM1	ITAG6	IL1A	CXCL12					

Table 7: Table of significantly differentially expressed genes and the pathways in which they are involved when comparing squamous cell in situ to invasive squamous cell carcinoma in organ transplant patients. Pathways with the highest global significance scores are indicated with *. Genes highlighted in pink are downregulated with pvalue<0.01. Genes highlighted in blue are upregulated with pvalue<0.05. Genes highlighted in green are downregulated with pvalue<0.05.

Comparison			
OTIS vs. all OTInv	Angiogenesis		
	Antigen Presentation	HLA-DRB5	
	Apoptosis		
	Autophagy		
	Cell Proliferation		
	Costimulatory Signaling	HLA-DRB5	CD70
	Cytokine and Chemokine Signaling		
	Cytotoxicity	SIRPA	
	DNA Damage Repair	MSH2	
	Epigenetic Regulation		
	Hedgehog Signaling		
	Hypoxia		
	Immune Cell Adhesion and Migration		
	Interferon Signaling	HLA-DRB5	
	JAK-STAT Signaling		
	Lymphoid Compartment		CD70
	MAPK	FAS	
	Matrix Remodeling and Metastasis	LOXL2	
	Metabolic Stress		
	Myeloid Compartment	SIRPA	
NF-kappaB Signaling	CD70	NFKBIE	
Notch Signaling			
PI3K-Akt			
TGF-beta Signaling			
Wnt Signaling			

Table 8: Table of significantly differentially expressed genes and the pathways in which they are involved when comparing normal skin to squamous cell in situ in organ transplant patients. Pathways with the highest global significance scores are indicated with *. Genes highlighted in pink are downregulated with pvalue<0.01. Genes highlighted in green are downregulated with pvalue<0.05.

Comparison			
	*	FGFR1	
Angiogenesis			
Antigen Presentation			
Apoptosis			
Autophagy			
Cell Proliferation			
Costimulatory Signaling			
Cytokine and Chemokine Signaling			
Cytotoxicity			
DNA Damage Repair			
Epigenetic Regulation			
Hedgehog Signaling			
Hypoxia			
Immune Cell Adhesion and Migration	*	NCAMI	
Interferon Signaling	*	NCAMI	
JAK-STAT Signaling			
Lymphoid Compartment			
MAPK		FGFR1	
Matrix Remodeling and Metastasis	*	NCAMI	
Metabolic Stress		FGFR1	
Myeloid Compartment			
NF-kappaB Signaling			
Notch Signaling			
PI3K-Akt		FGFR1	
TGF-beta Signaling			
Wnt Signaling			

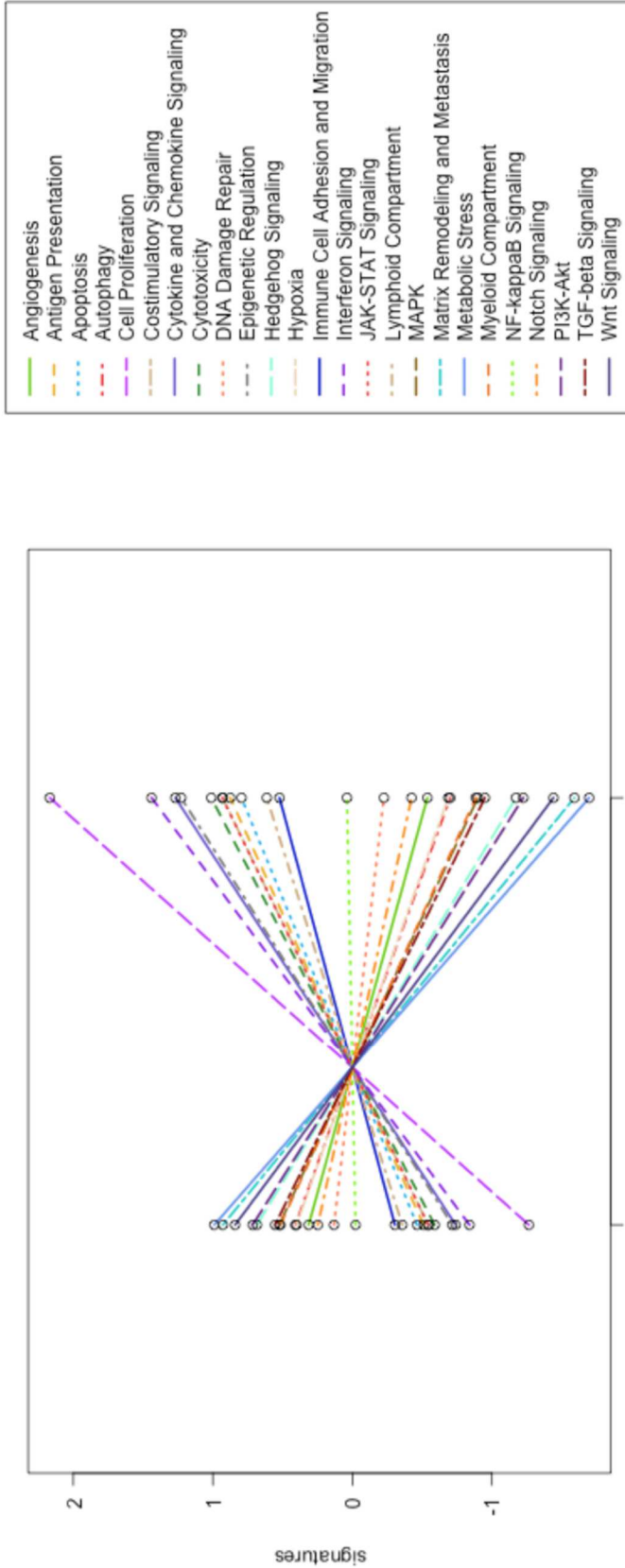
7. Supplemental Tables

Supplemental Table 1. Undirected global significance scores in SCC vs. BCC show that hedgehog signaling is the most differentially expressed gene set, whereas directed global significance scores show the most upregulated gene sets in SCC when compared to BCC are the myeloid compartment, interferon signaling, cytotoxicity, and antigen presentation, all of which fall under the panel's key immuno-oncology signature of anti-tumor immune activity and tumor immunogenicity. A high undirected global significance score takes into account both highly upregulated and highly downregulated genes within a gene set, whereas that same gene set may have a directed global significance score close to zero. A high directed global significance score only takes into account the gene sets where most of the genes are either only highly upregulated or only highly downregulated.

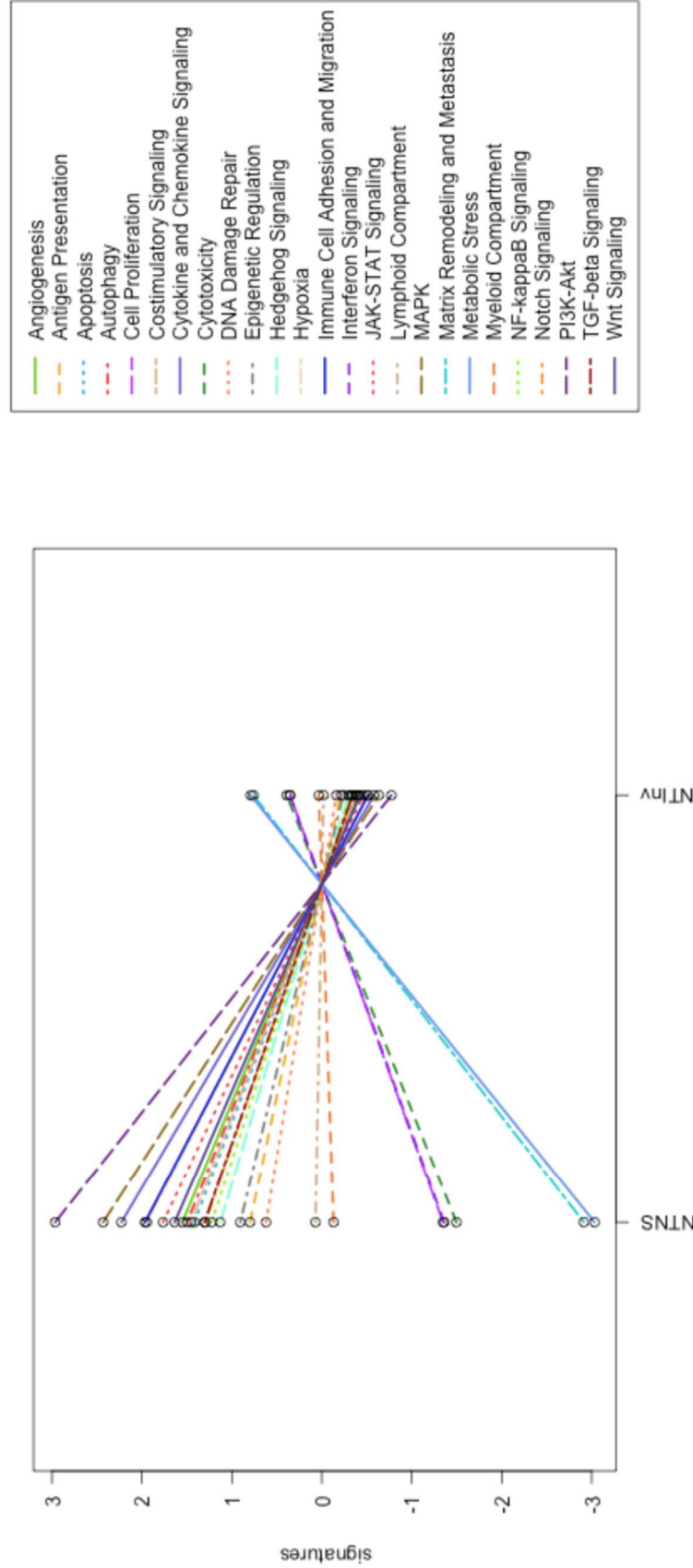
Gene Set	Undirected Global Significance scores: SCC	Gene Set	Directed Global Significance scores:
DNA Damage Repair	2.077	Epigenetic Regulation	-2.437
Epigenetic Regulation	2.561	Autophagy	-1.923
Cytokine and Chemokine Signaling	2.752	DNA Damage Repair	-1.436
Costimulatory Signaling	2.772	Hedgehog Signaling	0.443
Lymphoid Compartment	2.773	Cell Proliferation	1.983
Cell Proliferation	2.799	MAPK	2.008
Autophagy	3.043	Angiogenesis	2.26
JAK-STAT Signaling	3.051	JAK-STAT Signaling	2.332
Immune Cell Adhesion and Migration	3.064	Matrix Remodeling and Metastasis	2.335
MAPK	3.164	Cytokine and Chemokine Signaling	2.429
Angiogenesis	3.234	Costimulatory Signaling	2.548
Metabolic Stress	3.328	Lymphoid Compartment	2.576
Matrix Remodeling and Metastasis	3.389	Metabolic Stress	2.614
Cytotoxicity	3.426	Immune Cell Adhesion and Migration	2.681
Apoptosis	3.48	Apoptosis	2.818
Antigen Presentation	3.529	Hypoxia	2.96
Myeloid Compartment	3.627	Cytotoxicity	3.227
Interferon Signaling	3.741	Antigen Presentation	3.47
Hypoxia	3.899	Interferon Signaling	3.478
Hedgehog Signaling	4.388	Myeloid Compartment	3.585

8. Supplemental Figures

Supplemental Fig. 1: Plot of pathway score variation from non-transplant actinic keratosis to non-transplant squamous cell in situ shows increased expression in the majority of the genes that make up the cell proliferation pathway in squamous cell in situ compared to actinic keratosis. Colored lines show each pathway's average score from non-transplant actinic keratosis to non-transplant squamous cell in situ.



Supplemental Fig. 2: Plot of pathway score variation from non-transplant normal skin to non-transplant invasive squamous cell carcinoma shows increased expression in the majority of the genes that make up the matrix remodeling and metastasis, the metabolic stress, the cell proliferation, and the cytotoxicity pathways in invasive squamous cell carcinoma compared to normal skin. Colored lines show each pathways' average scores from non-transplant normal skin to non-transplant invasive squamous cell carcinoma



9. Bibliography

- Armanious, H., Adam, B., Meunier, D., Formenti, K., & Izevbaye, I. (2020). Digital gene expression analysis might aid in the diagnosis of thyroid cancer. *Current Oncology*, 27(2), e93.
- Ayers, M., Lunceford, J., Nebozhyn, M., Murphy, E., Loboda, A., Kaufman, D. R., Albright, A., Cheng, J.D., Kang, S.P., Shankaran, V., Piha-Paul, S.A., Yearley, J., Seiwert, T.Y., Ribas, A., & McClanahan, T. K. (2017). IFN- γ -related mRNA profile predicts clinical response to PD-1 blockade. *The Journal of clinical investigation*, 127(8), 2930-2940.
- Borden, E. S., Kang, P., Natri, H. M., Phung, T. N., Wilson, M. A., Buetow, K. H., & Hastings, K. T. (2019). Neoantigen fitness model predicts lower immune recognition of cutaneous squamous cell carcinomas than actinic keratoses. *Frontiers in Immunology*, 10, 2799.
- Boshuizen, J., Vredevoogd, D. W., Krijgsman, O., Ligtenberg, M. A., Blankenstein, S., de Bruijn, B., Frederick, D.T., Kenski, J.C., Parren, M., Brüggemann, M., Madu, M.F., Rozeman, E.A., Song, J., Horlings, H.M., Blank, C.U., van Akkooi, A.C.J., Flaherty, K.T., Boland, G.M., & Peeper, D. S. (2020). Reversal of pre-existing NGFR-driven tumor and immune therapy resistance. *Nature communications*, 11(1), 1-13.
- Brantsch, K. D., Meisner, C., Schönfisch, B., Trilling, B., Wehner-Caroli, J., Röcken, M., & Breuninger, H. (2008). Analysis of risk factors determining prognosis of cutaneous squamous-cell carcinoma: a prospective study. *The lancet oncology*, 9(8), 713-720.
- Cheng, P., Liu, H., & Gabrilovich, D. (2014). Notch Signaling in Differentiation and Function of Dendritic Cells. *Stem Cells and Cancer Stem Cells, Volume 12*, 77-88.
- Efremova, M., Finotello, F., Rieder, D., & Trajanoski, Z. (2017). Neoantigens Generated by Individual Mutations and their Role in Cancer Immunity and Immunotherapy. *Frontiers in Immunology*, 8, 1679.
- GeoMx Digital Spatial Profiler (DSP). (2021, May 25). Retrieved from <https://www.nanostring.com/products/geomx-digital-spatial-profiler/geomx-dsp-overview/>
- Gorbunova, A. S., Yapryntseva, M. A., Denisenko, T. V., & Zhivotovsky, B. (2020). BNIP3 in Lung Cancer: To Kill or Rescue?. *Cancers*, 12(11), 3390.
- Grose, R., & Dickson, C. (2005). Fibroblast growth factor signaling in tumorigenesis. *Cytokine & growth factor reviews*, 16(2), 179-186.
- Han, Y., Ren, J., Lee, E., Xu, X., Yu, W., & Muegge, K. (2017). Lsh/HELLS regulates self-renewal/proliferation of neural stem/progenitor cells. *Scientific reports*, 7(1), 1-14.

- Inman, G. J., Wang, J., Nagano, A., Alexandrov, L. B., Purdie, K. J., Taylor, R. G., Sherwood, V., Thomson, J., Hogan, S., Spender, L.C., South, A.P., Stratton, M., Chelala, C., Harwood, C.A., Proby, C.M., & Leigh, I. M. (2018). The genomic landscape of cutaneous SCC reveals drivers and a novel azathioprine associated mutational signature. *Nature communications*, 9(1), 1-14.
- Jamieson, N. B., & Maker, A. V. (2017). Gene-expression Profiling to Predict Responsiveness to Immunotherapy. *Cancer Gene Therapy*, 24(3), 134.
- Jennings, L., & Schmults, C. D. (2010). Management of High-Risk Cutaneous Squamous Cell Carcinoma. *The Journal of Clinical and Aesthetic Dermatology*, 3(4), 39.
- Karia, P. S., Han, J., & Schmults, C. D. (2013). Cutaneous Squamous Cell Carcinoma: Estimated Incidence of Disease, Nodal Metastasis, and Deaths from Disease in the United States, 2012. *Journal of the American Academy of Dermatology*, 68(6), 957-966.
- Karia, P. S., Jambusaria-Pahlajani, A., Harrington, D. P., Murphy, G. F., Qureshi, A. A., & Schmults, C. D. (2014). Evaluation of American Joint Committee on Cancer, International Union Against Cancer, and Brigham and Women's Hospital tumor staging for cutaneous squamous cell carcinoma. *Journal of Clinical Oncology*, 32(4), 327.
- Khandelwal, A. R., Kent, B., Hillary, S., Alam, M. M., Ma, X., Gu, X., DiGiovanni, J., & Nathan, C. A. O. (2019). Fibroblast growth factor receptor promotes progression of cutaneous squamous cell carcinoma. *Molecular carcinogenesis*, 58(10), 1715-1725.
- Kryczek, I., Peng, D., Nagarsheth, N. B., Zhao, L., Wei, S., Zhao, E., Vatan, L., Szeliga, W., Liu, R., Kotarski, J., Tarkowski, R., Wang, W., & Zou, W. (2016). Epigenetic silencing of TH1-type chemokines shapes tumour immunity and immunotherapy.
- Lee, C. H., Yelensky, R., Jooss, K., & Chan, T. A. (2018). Update on Tumor Neoantigens and Their Utility: Why It Is Good to Be Different. *Trends in Immunology*, 39(7), 536-548.
- Li, Y. Y., Hanna, G. J., Laga, A. C., Haddad, R. I., Lorch, J. H., & Hammerman, P. S. (2015). Genomic analysis of metastatic cutaneous squamous cell carcinoma. *Clinical cancer research*, 21(6), 1447-1456.
- Migden, M. R., Rischin, D., Schmults, C. D., Guminski, A., Hauschild, A., Lewis, K. D., Chung, C.H., Hernandez-Aya, L., Lim, A.M., Chang, A.S., Rabinowits, G., Thai, A.A., Dunn, L.A., Hughes, B.G.M., Khushalani, N.I., Modi, B., Schadendorf, D., Gao, B., Seebach, F., Li, S., Li, J., Mathias, M., Booth, J., Mohan, K., Stankevich, E., Babiker, H.M., Brana, I., Gil-Martin, M., Homsí, J., Johnson, M.L., Moreno, V., Niu, J., Owonikoko, T.K., Papadopoulos, K.P., Yancopoulos, G.D., Lowy, I., & Fury,

- M.G. (2018). PD-1 Blockade with Cemiplimab in Advanced Cutaneous Squamous-Cell Carcinoma. *New England Journal of Medicine*, 379(4), 341-351.
- Ng, Y. Z., Dayal, J. H., & South, A. P. (2011). Genetic Predisposition to Cutaneous Squamous Cell Carcinoma. In *Skin Cancers-Risk Factors, Prevention and Therapy*. Retrieved from <http://www.intechopen.com/books/skin-cancers-risk-factors-prevention-and-therapy/genetic-predisposition-to-cutaneous-squamous-cell-carcinoma>
- Padilla, R. S., Sebastian, S., Jiang, Z., Nindl, I., & Larson, R. (2010). Gene expression patterns of normal human skin, actinic keratosis, and squamous cell carcinoma: a spectrum of disease progression. *Archives of dermatology*, 146(3), 288-293.
- Rizvi, N. A., Hellmann, M. D., Snyder, A., Kvistborg, P., Makarov, V., Havel, J. J., Lee, W., Yuan, J., Wong, P., Ho, T.S., Miller, M.L., Rekhtman, N., Moreira, A.L., Ibrahim, F., Bruggeman, C., Gasmir, B., Zappasodi, R., Maeda, Y., Sander, C., Garon, E.B., Merghoub, T., Wolchok, J.D., Schumacher, T.N., & Chan, T.A. (2015). Mutational Landscape Determines Sensitivity to PD-1 Blockade in Non-Small Cell Lung Cancer. *Science*, 348(6230), 124-128.
- Robinson, M. H., Maximov, V., Lallani, S., Farooq, H., Taylor, M. D., Read, R. D., & Kenney, A. M. (2019). Upregulation of the chromatin remodeler HELLS is mediated by YAP1 in Sonic Hedgehog Medulloblastoma. *Scientific reports*, 9(1), 1-15.
- Salas-Benito, D., Conde, E., Tamayo-Uria, I., Mancheño, U., Elizalde, E., Garcia-Ros, D., Aramendia, J.M., Muruzabal, J.C., Alcaide, J., Guillen-Grima, F., Minguez, J.A., Amores-Tirado, J., Gonzalez-Martin, A., Sarobe, P., Lasarte, J.J., Ponze-Sarvisé, M., De Andrea, C.E., & Hervas-Stubbs, S. (2021). The mutational load and a T-cell inflamed tumour phenotype identify ovarian cancer patients rendering tumour-reactive T cells from PD-1+ tumour-infiltrating lymphocytes. *British journal of cancer*, 124(6), 1138-1149.
- Schoenberger, S. P. (2017). Is It Possible to Develop Cancer Vaccines to Neoantigens, What Are the Major Challenges, and How Can These Be Overcome? Targeting the Right Antigens in the Right Patients. *Cold Spring Harbor Perspectives in Biology*, 10(11), 1.
- Schumacher, T. N., & Schreiber, R. D. (2015). Neoantigens in cancer immunotherapy. *Science*, 348(6230), 69-74.
- Skhinas, J. N., & Cox, T. R. (2018). The interplay between extracellular matrix remodelling and kinase signalling in cancer progression and metastasis. *Cell adhesion & migration*, 12(6), 529-537.
- Spranger, S., & Gajewski, T. F. (2018). Impact of oncogenic pathways on evasion of antitumour immune responses. *Nature Reviews Cancer*, 18(3), 139.

- Sugita, H., Iida, S., Inokuchi, M., Kato, K., Ishiguro, M., Ishikawa, T., Takagi, Y., Enjoji, M., Yamada, H., Uetake, H., Kojima, K., & Sugihara, K. (2011). Methylation of BNIP3 and DAPK indicates lower response to chemotherapy and poor prognosis in gastric cancer. *Oncology reports*, *25*(2), 513-518.
- Vara-Pérez, M., Rossi, M., Van den Haute, C., Maes, H., Sassano, M. L., Venkataramani, V., Michalke, B., Romano, E., Rillaerts, K., Garg, A.D., Schepkens, C., Bosiso, F.M., Wouters, J., Oliveira, A.I., Vangheluwe, P., Annaert, W., Swinnen, J.V., Colet, J.M., van den Oord, J.J., Fendt, S.M., Mazzone, M., & Agostinis, P. (2021). BNIP3 promotes HIF-1 α -driven melanoma growth by curbing intracellular iron homeostasis. *The EMBO journal*, *40*(10), e106214.
- Walter, A., Barysch, M. J., Behnke, S., Dziunycz, P., Schmid, B., Ritter, E., Gnjjatic, S., Kristiansen, G., Moch, H., Knuth, A., Dummer, R., & van den Broek, M. (2010). Cancer-testis antigens and immunosurveillance in human cutaneous squamous cell and basal cell carcinomas. *Clinical Cancer Research*, *16*(14), 3562-3570.
- Wang, N. J., Sanborn, Z., Arnett, K. L., Bayston, L. J., Liao, W., Proby, C. M., Leigh, I.M., Collisson, E.A., Gordon, P.B., Jakkula, L., Pennypacker, S., Zou, Y., Sharma, M., North, J.P., Vemula, S.S., Mauro, T.M., Neuhaus, I.M., LeBoit, P.E., Hur, J.S., Park, K., Huh, N., Kwok, P.Y., Arron, S.T., Massion, P.P., Bale, A.E., Haussler, D., Cleaver, J.E., Gray, J.W., Spellman, P.T., South, A.P., Aster, J.C., Blacklow, S.C., & Cho, R. J. (2011). Loss-of-function mutations in Notch receptors in cutaneous and lung squamous cell carcinoma. *Proceedings of the National Academy of Sciences*, *108*(43), 17761-17766.
- Yang, X. P., Jiang, K., Hirahara, K., Vahedi, G., Afzali, B., Sciume, G., Bonelli, M., Sun, H.W., Jankovic, D., Kanno, Y., Sartorelli, V., O'Shea, J.J., & Laurence, A. (2015). EZH2 is crucial for both differentiation of regulatory T cells and T effector cell expansion. *Scientific reports*, *5*(1), 1-14.
- Zingg, D., Arenas-Ramirez, N., Sahin, D., Rosalia, R. A., Antunes, A. T., Haeusel, J., Sommer, L., & Boyman, O. (2017). The histone methyltransferase Ezh2 controls mechanisms of adaptive resistance to tumor immunotherapy. *Cell reports*, *20*(4), 854-867.
- nCounter*® *Advanced Analysis Software*. NanoString. (2021, April 5).
<https://www.nanostring.com/products/analysis-solutions/ncounter-advanced-analysis-software/>.
- nCounter*® *PanCancer IO 360*™ *Panel*. NanoString. (2021, June 14).
<https://www.nanostring.com/products/ncounter-assays-panels/oncology/pancancer-io-360/>.